Available online at www.sciencedirect.com
ScienceDirect
Ceramics International 35 (2009) 741–745
CERAMICS INTERNATIONAL
www.elsevier.com/locate/ceramint

Correlation between microstructure and mechanical properties of Al_2O_3/ZrO_2 nanocomposites

Francisco A.T. Guimarães [a], Kátia L. Silva [a], Vania Trombini [a], Juliano J. Pierri [b], José A. Rodrigues [b], Roberto Tomasi [b], Eliria M.J.A. Pallone [a,*]

[a] *Universidade São Francisco – PPG-Engenharia e Ciência dos Materiais, Rua Alexandre Rodrigues Barbosa, 45 – 13251-900 Itatiba, SP, Brazil*
[b] *Universidade Federal de São Carlos, Departamento de Engenharia de Materiais – cp 676, 13.565-905, São Carlos, SP, Brazil*

Received 12 September 2007; received in revised form 5 December 2007; accepted 7 February 2008
Available online 4 June 2008

Abstract

The aim of this work was to correlate the microstructure of alumina matrix nanocomposites containing 1, 3, and 5 vol% of monoclinic zirconia nanometric particles with the mechanical properties and wear resistance of these composites. The microstructural analysis showed the beneficial effect of the zirconia particles in the alumina matrix regarding grain growth and improvement of the properties: up to 8% for the microhardness, 11% for the flexural strength and 23% for the wear resistance for nanocomposites containing 5 vol% of particles when compared to inclusion-free alumina.

Keywords: A. Sintering; B. Nanocomposites; C. Mechanical properties; D. Al_2O_3/ZrO_2; E. Wear parts

1. Introduction

High performance ceramic matrix structural composites have been developed nowadays aiming to take advantage from nanostructures. Among the main studied composites, the systems with alumina matrix containing nanometric inclusions of SiC, TiC, ZrO_2, and NbC can be highlighted [1–11].

Ceramic nanocomposites show improved mechanical properties compared to materials without reinforcement caused by mechanisms associated to the presence of nanoparticles. Among the proposed systems, the Al_2O_3/SiC nanocomposite is one of the most important for its highly improved mechanical properties [12]. The existence of residual stresses caused by the difference in thermal expansion coefficients of Al_2O_3 ($\approx 8 \times 10^{-6}\,K^{-1}$) and SiC ($\approx 4.2 \times 10^{-6}\,K^{-1}$) is the basis to explain such improvement. These stresses appear during cooling and cause the fracture mode of the material to change from intergranular to transgranular; thus the fracture toughness increases, since the energy needed to cause crack propagation trough the grains is higher than the one needed to cause crack propagation through grain boundaries [3]. The increase in flexural strength may be due to the reduction in the size of the material critical defects and to the reduction in surface defects [7–13]. The main objective of this work was to study the effect of ZrO_2 nanometric inclusions in the processing of Al_2O_3/ZrO_2 nanocomposites and to correlate their microstructure with both mechanical strength and wear resistance.

2. Materials and methods

The materials used for the preparation of the nanocomposites were commercial alumina (Al_2O_3 – purity 99.995%; mean particle diameter 0.2 μm; specific surface area 13.6 m^2/g) AKP-53 provided by Sumitomo Co., Japan, and commercial nanometric zirconia (ZrO_2 – purity 99.9%; monoclinic, and surface area 19.8 m^2/g), provided by Nanostructured Materials Inc. As-received zirconia was characterized by X-ray diffraction (XRD – Siemens diffractometer, model 5100, with radiation $K\alpha_{(Cu)}$) which measured the size of the crystallite using the Sherrer formula, particle size distribution (Sedigrah 5100 – Micromeritics), specific surface area (BET, Gemini 2370 – Micromeritics), high-resolution scanning electron

* Corresponding author. Tel.: +55 11 45348059; fax: +55 11 45241933.
E-mail address: eliria.pallone@saofrancisco.edu.br (E.M.J.A. Pallone).

0272-8842/$34.00
doi:10.1016/j.ceramint.2008.02.002

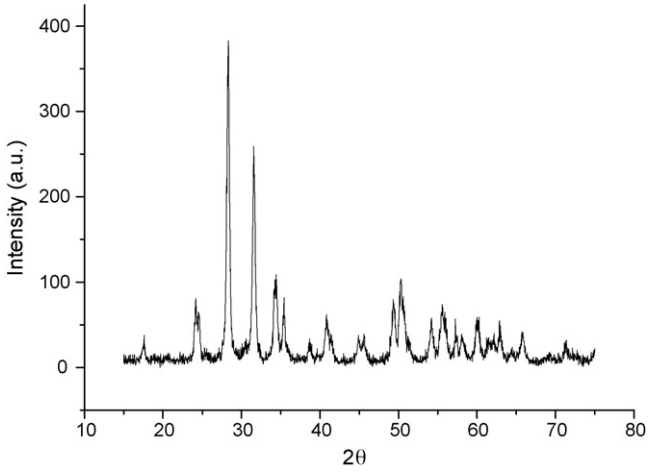

Fig. 1. X-ray diffractogram of zirconia powder.

microscopy (SEM – Phillips FEG XL30), and transmission electron microscopy (TEM – Phillips CM120, 120 kV).

In order to disperse the ZrO_2 particles into the Al_2O_3 matrix, a suspension of ZrO_2 with 0.5 wt.% of aminobenzoic acid (PABA – used as deflocculant) in alcohol was used. The suspension was obtained in a ball-mill with ball-to-powder ratio of 4:1. After 12 h of grinding, the resulting slip was separated by grinding means and stored. Simultaneously, a suspension of Al_2O_3 in alcoholic media was also prepared. In this case, 0.2 wt.% of PABA was added, and the suspension was ground in a ball-to-powder mill of 5:1 during 1 h. The zirconia suspension previously prepared was then added to the alumina suspension, in order to obtain volumetric proportions of 1, 3, and 5 vol% of ZrO_2 in the alumina matrix [14,15]. The final suspension was mixed in a ball-mill during 22 h, followed by addition of 0.5 wt.% of oleic acid and two more hours of mixing. The resulting mixture was dried in airflow and sieved through 80-mesh, to eliminate coarse agglomerates.

The obtained powders were uniaxially pressed and isostatically shaped in 10 mm diameter and about 5 mm height discs (to make the dilatometry tests), in bars with approximate dimensions of 4.2 mm × 4.7 mm × 27.5 mm (to be used in the flexural tests), and in about 6.7 mm diameter and 12 mm height pins (to make the wear tests). After forming, a pre-treatment at 500 °C in air during 3 h was carried out in order to eliminate organic compounds from grounding and processing additives.

Table 1
Mean particle size (D_{50}) and specific surface area (SSA) of zirconia powder

Sample	D_{50} (nm)	SSA (m^2/g)
Commercial zirconia	100.00	20.00

Dilatometry tests were carried out to determine the temperature ranges of shrinkage beginning at a maximum shrinkage rate in order to optimize the sintering process. From these results, the specimens containing 0, 1, 3, and 5 vol% of ZrO_2 were sintered at 1390, 1420, 1440, and 1460 °C, respectively, for 2 h with a heating rate of 10 °C/min.

To analyze the microstructure, specimens were polished and thermally etched. The analysis was carried out in a scanning electron microscope Phillips-XL30-FEG. Vickers microhardness measurements were realized with a microhardness equipment, Buehler, with a diamond indenter using a load of 200 g. Three-point flexural strength was measured with an INSTRON equipment, model 1127, with velocity test of 0.2 mm/min using span of 20 mm, as described in the ASTM C1161-94 standard [16]. Specimens were also characterized in terms of wear by the ''pin on disc'' test, in a PLINT device, model TE67. The applied load was 33 N and the sliding distance was 3000 m.

3. Results and discussion

Fig. 1 shows a XRD spectrum of the as-received zirconia powder. All the observed peaks refer to the monoclinic zirconia. Using the Scherrer formula, it was possible to calculate the size of the crystallite, obtaining 27 nm, which was determined from the XRD patterns using the width of the Bragg reflection profiles at half of the maximum intensity.

Table 1 shows the particle size values, given by the spherical equivalent diameter for accumulated mass of 50% (D_{50}) and the specific surface area (SSA) of zirconia powder. Crystallite size (27 nm), SSA, and spherical diameter are reasonably close to the primary particles size observed in the micrograph shown in Fig. 2, which is 50 nm. On the other hand, even tough the value

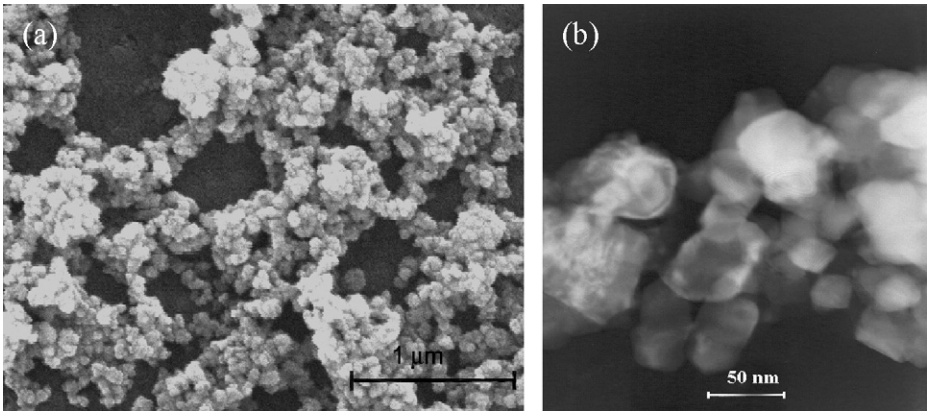

Fig. 2. Micrograph obtained by: (a) scanning electron microscopy and (b) transmission electron microscopy of as-received zirconia powder.

Table 2
Green density (GD) and apparent density (AD) of alumina samples with 0, 1, 3, and 5 vol% of nanometric ZrO_2. Theoretical density (TD) values are also showed

Percentage of ZrO_2 in the alumina matrix (in vol)	0% ZrO_2	1% ZrO_2	3% ZrO_2	5% ZrO_2
GD (%DT)	60.6 ± 0.3	60.7 ± 0.4	64.4 ± 0.4	64.7 ± 0.3
AD (%DT)	99.6 ± 0.2	98.9 ± 0.3	98.3 ± 0.4	98.0 ± 0.3
TD (g/cm^3)	3.98	3.99	4.02	4.04

of D_{50} is below the detection limits of the employed measuring method (sedimentation), it can be interpreted as an indication that the primary particles were not completely dispersed throughout the test suspension. It can also be observed from Fig. 2 that the as-received zirconia powder agglomerates. Grinding and mixture with alumina must eliminate these agglomerates.

Table 2 shows the green density (GD) and apparent density (AD) values after sintering of samples containing 0, 1, 3, and 5 vol% of ZrO_2 given as percentage of theoretical density (TD). It can be observed that the green density rises when zirconia amount is increased. This can be attributed to the higher powder packing caused by the presence of nanometric zirconia, which occupies part of the voids among alumina particles.

Fig. 3(a) and (b) shows the shrinkage rate curves of alumina samples with additions of 0, 1, 3, and 5 vol% of zirconia, which were used to determine the best sintering temperature for each composition. It is observed that the maximum shrinkage rate occurred at different temperatures for each composition. The maximum shrinkage rate for the compositions containing 0, 1, 3, and 5 vol% of zirconia occurred at 1390, 1420, 1440, and 1460 °C, respectively.

As presented before, Table 2 shows the apparent density of sintered samples for optimal conditions of sintering. Even with nanometric dimensions of zirconia and green density increase, densification of sintered samples decreased with zirconia content. This decrease may occur because of the agglomerating of zirconia powder that could not be eliminated during the powder processing step. These agglomerates lead to the formation of coarse zirconia grains, as can be seen in the micrography shown in Fig. 4, for the system with 5 vol% of zirconia. Even with these agglomerates, it was possible to obtain more dense samples when compared to similar materials reported in the literature [4–9].

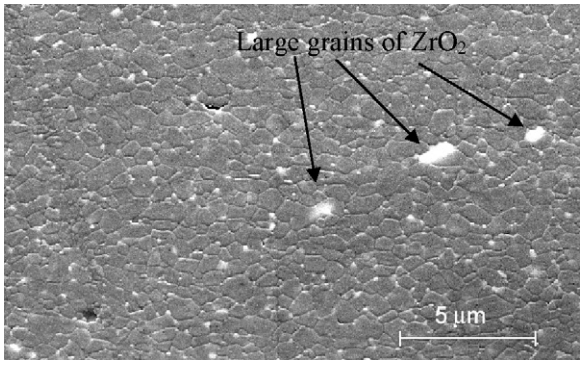

Fig. 4. Micrograph of the composite Al_2O_3–5 vol% of ZrO_2, in which coarse grains of ZrO_2 formed by particles agglomeration can be seen.

Fig. 5(a) and (b) shows micrographs of alumina and alumina with 1 vol% of ZrO_2 samples, respectively. The presence of zirconia particles on the grain boundaries (white spots) suggests that they inhibit the alumina grain growth, even with such low content of them. It was verified that the mean grain size of zirconia-free alumina samples is around 1.21 ± 0.33 μm, while for the sample with 1 vol% of zirconia the mean grain size decreased to 0.68 ± 0.12 μm. This result confirms the pinning effect of zirconia inclusions on alumina grain boundaries.

Fig. 6 shows the micrographs of the alumina nanocomposite with 3 vol% of ZrO_2. It can be observed that the inclusions are also located on the grain boundaries, and lots of them are on triple points. This location was similar to those shown by alumina/SiC composites [9,10].

In the presented case, the zirconia particles are dispersed mainly on the grain boundaries, resulting in an intergranular type nanocomposite, while for the silicon carbide, the inclusions appear both on grain boundaries and inside the

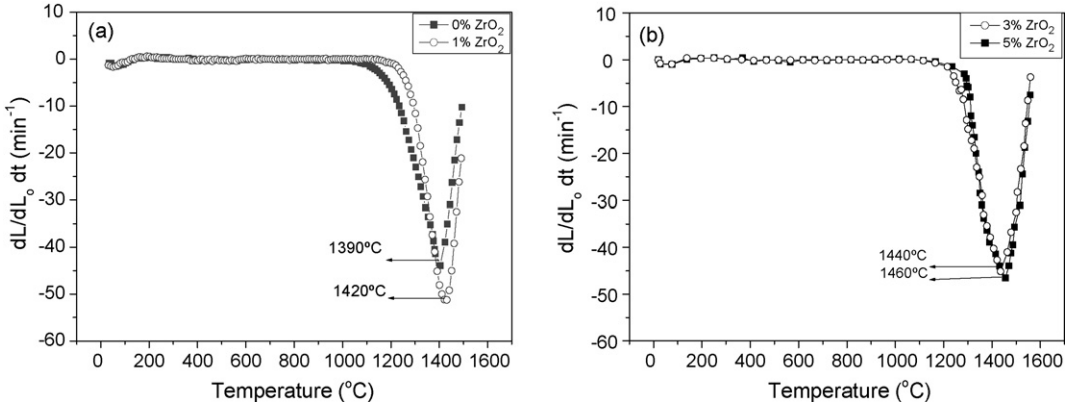

Fig. 3. Curves of shrinkage rate of samples of (a) Al_2O_3 with 0 and 1 vol% ZrO_2, and (b) Al_2O_3 with 3 and 5 vol% ZrO_2.

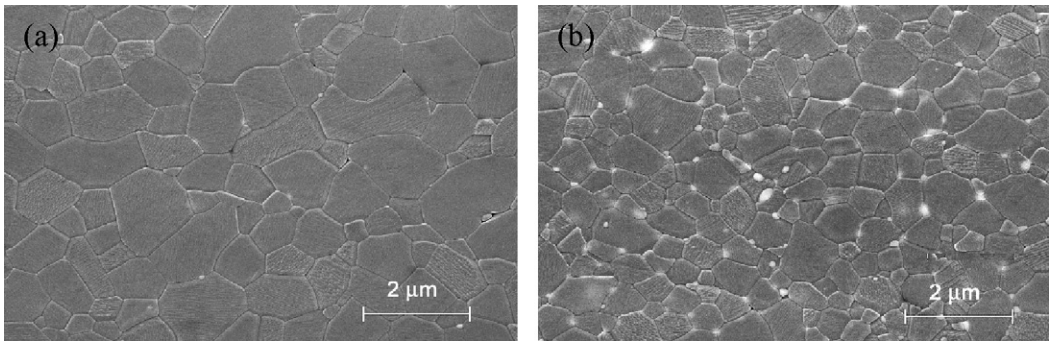

Fig. 5. Micrographies of alumina: (a) without ZrO_2 and (b) with 1 vol% of ZrO_2.

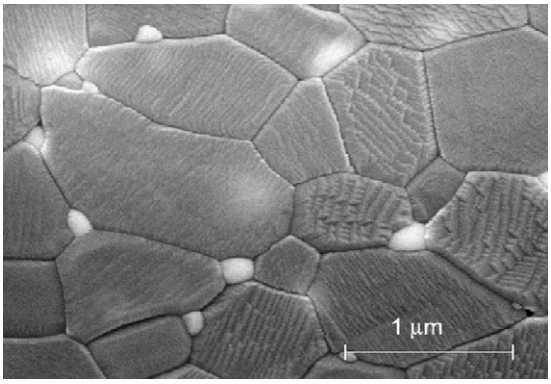

Fig. 6. Micrography of the alumina nanocomposite with 3 vol% of ZrO_2.

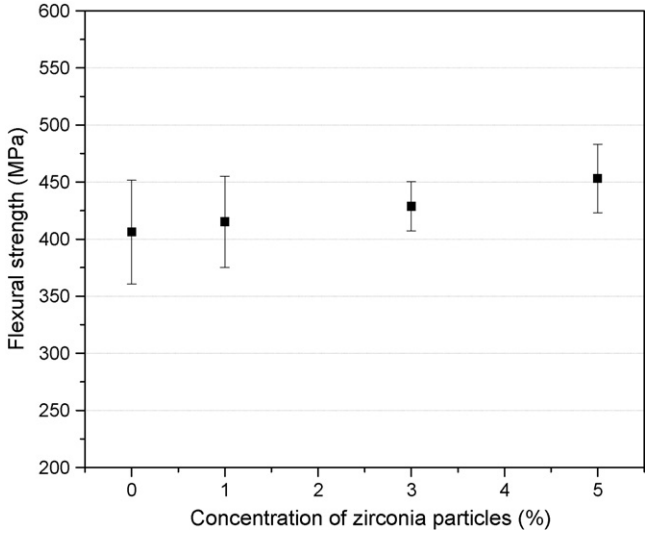

Fig. 7. Three-point flexural strength of the nanocomposites as a function of the nanometric zirconia concentration.

Table 3
Vickers microhardness values of the sample Al_2O_3 with 0, 1, 3 and 5 vol% ZrO_2

Sample	Hardness (GPa)
Al_2O_3 + 0 vol% ZrO_2	19.39 + 0.80
Al_2O_3 + 1 vol% ZrO_2	19.77 + 0.62
Al_2O_3 + 3 vol% ZrO_2	20.82 + 0.96
Al_2O_3 + 5 vol% ZrO_2	21.01 + 0.40

grains, forming a nanocomposite of the intra/intergranular type [3]. Since there is grain growth in the matrix, even the zirconia inclusions making it more difficult, and these inclusions having bigger dimensions than the original ones, as shown in Fig. 6, the mechanism that controls matrix grain growth in the presence of zirconia inclusions could be different from that observed for silicon carbide inclusions [9].

Fig. 7 shows the results of the three-point bending tests as a function of the concentration of zirconia particles in the alumina matrix. Despite the errors associated to these measurements, it is observed that the mean values of mechanical strength increase with zirconia concentration. The obtained strength for zirconia-free alumina shows that the processing steps were suitable in order to achieve higher flexural strength compared to the values reported in the literature for similar systems [8–11].

Table 3 shows the results of microhardness obtained for Al_2O_3 and for alumina nanocomposites containing 1, 3, and 5 vol% of ZrO_2. It is observed that inclusion of zirconia in the alumina matrix increases hardness.

Fig. 8 shows the wear rate of the composites as a function of the concentration of zirconia particles. It is observed that the wear rate decreases when zirconia is added. Comparing the

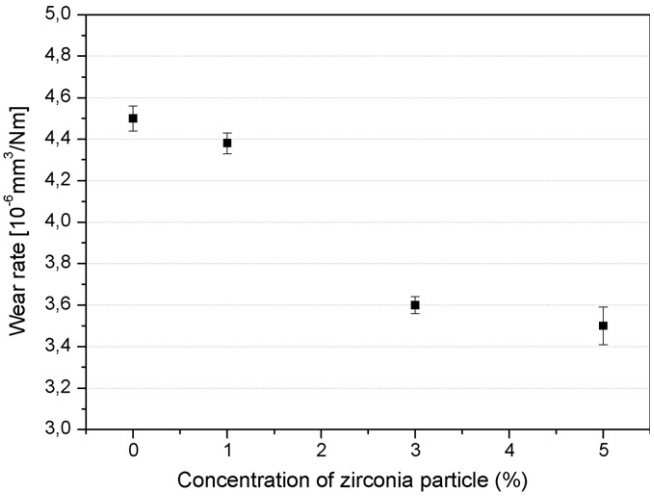

Fig. 8. Wear rate of the nanocomposites as a function of the zirconia particles concentration.

wear rate of zirconia-free alumina to alumina with 5% in volume of zirconia, it is verified that the wear rate decreases about 23% for this nanocomposite. One possible explanation for this phenomenon can be related to the inclusions that make grain detaching harder during the initial surface wear steps [17–19].

4. Conclusions

The addition of nanometric zirconia particles in the alumina matrix to enhance mechanical properties of this system, when compared to inclusion-free alumina, proved efficient. Low additions of zirconia (1 vol%) are enough to inhibit the grain growth of alumina, making the refinement of the microstructure possible. The mechanical properties of the Al_2O_3/ZrO_2 composite improved with the increase of the concentration of nanometric zirconia inclusions compared to alumina without zirconia. The hardness of the Al_2O_3 nanocomposite containing 5 vol% of ZrO_2 was 21 GPa, and its flexural strength was 450 MPa. Finally, the wear rate of this same nanocomposite is lower compared to the zirconia-free alumina, 3.5×10^{-6} and 4.5×10^{-6} mm^3/Nm, respectively.

Acknowledgements

The authors are grateful for financial support from Brazilians Institutions FAPESP, CAPES and CNPq.

References

[1] A.L. Greer, Nanostructured materials—from fundamental to application, Mater. Sci. Forum 269–272 (1998) 3–10.
[2] K. Niihara, New design of structural ceramics—ceramic nanocomposites, J. Ceram. Soc. Jpn. 99 (10) (1991) 974–982.
[3] A. Nakahira, K. Niihara, Sintering behavior and consolidation process for Al_2O_3/SiC nanocomposites, J. Ceram. Soc. Jpn. 100 (4) (1992) 448–453.
[4] W.A. Tuan, R.Z. Chen, T.C. Wang, C.H. Cheng, P.S. Kuo, Mechanical properties of Al_2O_3/ZrO_2 composites, J. Eur. Ceram. Soc. 22 (2002) 2827–2833.
[5] E.M.J.A. Pallone, V. Trombini, W.J. Botta, R. Tomasi, Synthesis of Al_2O_3–NbC by reactive milling and production of nanocomposite, J. Mater. Process Technol. 143 (144) (2003) 185–190.
[6] W.J. Botta, R. Tomasi, E.M.J.A. Pallone, A.R. Yavari, Nanostructured composites obtained by reactive milling, Scripta Mater. 44 (2001) 1735–1740.
[7] R.J. Brook, R.A.D. Mackenzie, Nanocomposite materials, Compos. Mater. (1993) 27–30.
[8] G.J. Liu, H.B. Qui, R. Tood, R.J. Brook, J.K. Guo, Processing and mechanical behavior of Al_2O_3/ZrO_2 nanocomposite, Mater. Res. Bull. 33 (2) (1998) 281–288.
[9] L.C. Stearns, J. Zhao, M.P. Harmer, Processing and microstructure development in Al_2O_3–SiC nanocomposites, J. Eur. Ceram. Soc. 10 (1992) 473–477.
[10] A.H. De Aza, J. Chevalier, G. Fantozzi, Slow-crack-growth behavior of zirconia-toughened alumina ceramics processed by different methods, J. Am. Ceram. Soc. 86 (1) (2003) 115–120.
[11] J. Chevalier, S. Deville, G. Fantozzi, J.F. Bartolomé, C. Pecharroman, J.S. Moya, L.A. Diaz, R. Torrecillas, Nanostructured ceramic oxides with a slow crack growth resistance close to covalent materials, Nanoletters 5 (7) (2005) 1297–1301.
[12] C.E. Borsa, N.M.R. Jones, R.J. Brook, R.I. Todd, Influence of processing on the development and flexure strength of Al_2O_3/SiC nanocomposites, J. Eur. Ceram. Soc. 17 (1997) 865–872.
[13] M. Sternitzke, Structural ceramic nanocomposites, J. Eur. Ceram. Soc. 17 (1997) 1061–1082.
[14] J.J. Pierre, S.C. Maestrelli, E.M.J.A. Pallone, R. Tomasi, Cerâmica 51 (317) (2005) 8–12.
[15] E.M.J.A. Pallone, J. Pierre, V. Trombini, R. Tomasi, Production of Al_2O_3 nanocomposites with inclusions of nanometric ZrO_2, in: Proceedings of the Fourth International Conference on Science, Technology and Applications of Sintering, vol. 1, Grenoble, France, (2005), pp. 504–505.
[16] Annual book of standards, standard test method for flexural of advanced ceramics at ambient temperature, C1161-94, 1994.
[17] G.A. Carter, A.V. Riessen, R.D. Hart, Wear of zirconia-dispersed alumina at ambient temperature, 140 °C and 250 °C, J. Eur. Ceram. Soc. 26 (16) (2006) 3547–3555.
[18] H.J. Chen, W.M. Rainforth, W.E. Lee, The wear behaviour of Al_2O_3–SiC ceramic nanocomposite, Scripta Mater. 42 (2000) 555–560.
[19] F. Xiong, R.R. Manory, The effect of test parameters on alumina wear under low contact stress, Wear 236 (1999) 240–245.